Chapter 11

# Characterization of Intermetallic Precipitates in Ni-Base Alloys by Non-destructive Techniques

V. Acharya, S. Ramesh and G.V.S. Murthy

Additional information is available at the end of the chapter

http://dx.doi.org/10.5772/61119

**Abstract**

The present industrial scenario requires all engineering structure to be designed considering stability of several parameters at the operating conditions (e.g. Temperature, pressure, resistance to mechanical and surface degradation). Choice of materials for any engineering component should be such that it operates safely for reliable function, without failure during in-service, giving optimum component life. Due to scarcity of various resources and cost of manufacturing, regular maintenance and evaluation of structural integrity at every stage of production is necessary. Non-destructive techniques (NDT), along with modern computational facility help in non-intrusive investigation of the component at regular intervals of the operating stages for many critical applications. This will result in increment of designed component life and also help in maximizing utilization of natural resources.

For long, Ultrasonic has been associated with defect detection, but with the recent advances in electronics in combination with computational capabilities Ultrasonic velocity measurements have also been attempted for characterization of solutionising and precipitation behavior in various alloy systems such as aluminium alloys, ferritic steel, maraging steel, nickel base alloys and titanium alloys. As the speed of sound in a homogeneous medium is directly related to both elastic modulus and density, any changes in elastic property with varying degree of inhomogeneities will affect in pulse transit time through a sample of given thickness. Due to variation in elastic modulus of the matrix in the alloy resulting from the various precipitates; it has been attributed towards the change in ultrasonic velocity of the alloy and thereby resulting in popularization of Ultrasonic testing for online monitoring of the component. The precipitation hardening has been believed to arise from the formation of very small solute clusters which uses significant scattering of the conduction electron cause

during the rearrangement, while the formation of the precipitates; resulting in variation of electrical resistivity of the aged alloy.

In the present chapter, a few non-destructive techniques used to characterize different microstructural features and the precipitation behavior, evolved through various heat treatments using Direct Current Potential Drop (DCPD) technique for measuring electrical resistivity and Ultrasonic Testing for measurements of ultrasonic parameters are presented. Further, validation of the observed results on microstructural features is also presented through hardness and microscopy studies.Thus, this study in effect can be used for non-destructive evaluation of the microstructures.

**Keywords:** Inconel 718, Nimonic 263, Ageing, Intermetallic Precipitation, DC Electrical Resistivity, Ultrasonic Velocity, Hardness

## 1. Introduction

High-temperature materials are materials that possess a remarkable ability to maintain their properties at elevated temperatures. Special steels, lighter alloys, ceramics and composites can be used as high-temperature material, but due to lack of one or the other property, their application over a wide range of temperature is restricted. To achieve this step change in operating parameters, new high-temperature materials must be selected due to inherent limitations in steels. Thus, need for stronger and corrosion-resistant materials for high-temperature engineering resulted in development of "Superalloys" of "Stainless Steel" varieties. Superalloys are unique high-temperature materials that have an ability to retain most of their strength even after long exposure times above 650°C (923 K) along with good low-temperature ductility and excellent resistance to mechanical and chemical degradation in severe environments. High-temperature strength in Superalloys is due to the presence of a stable matrix having an austenitic face-centered cubic crystal (FCC) structure helping in the strengthening mechanism. The primary application of such alloys is in severe operating conditions, for example, space shuttle engine and gas turbines, which are subjected to both high temperature and pressures, alongwith corrosive environments [1,2].

The major constituents of Superalloys [1-4] are mostly group VIIIB elements from the transition metal and they consist of various combinations such as Fe, Ni, Co and Cr, as well as small amounts of W, Mo, Ta, Nb, Ti and Al. Depending on the base metal, these can be Nickel-based, Cobalt-based and Nickel-Iron-based Superalloys. Nickel-based alloys are the most complex, most widely used for the hottest parts and most preferred [5] Superalloy. Nickel-based Superalloys, used in vast applications, are mainly subjected to high temperature due to the principle characteristic of Ni as an alloy base having high phase stability of FCC nickel matrix along with strength retention upto 0.7 Tm (Tm – melting temperature). Diffusion rate of Ni is very low which leads to microstructural stability in the alloy at elevated temperatures. Co-based alloys have higher melting points than Ni and Ni-Fe based alloys, which gives them the

http://dx.doi.org/10.5772/61119

ability to absorb stress at a higher absolute temperature. Higher chromium content in Co alloys gives superior hot corrosion resistance to gas turbine atmospheres and also shows superior thermal fatigue resistance and weldability over Ni-alloys [1,2]. Superalloys containing substantial quantities of both Ni and Fe form a distinct class of Superalloys known as Nickel–Iron-based Superalloy. The austenitic FCC matrix of Superalloys has extended solubility for some alloying elements, excellent ductility and favorable characteristics for precipitation of effective strengthening phases. Superalloy density [2] is influenced by alloying additions: aluminum, titanium and chromium reduce density, whereas tungsten, rhenium and tantalum increase it. The corrosion resistance of Superalloys depends primarily on the alloying elements added, particularly chromium and aluminum, and the environment experienced.

Superalloys were thus developed to improve high-temperature strength along with other mechanical properties. Strengthening is a phenomenon by which hardness, yield and tensile strength are increased. Superalloys utilize three basic mechanisms [6] for strengthening: intermetallic precipitation, solid solution and carbide precipitation. Intermetallic and carbide precipitation are employed in a metastable condition and thus the basic structure and distribution of the phases alter on normal thermal exposures. Thermal exposures also increase the possibility [3,4] of phase alterations such as the formation of delta, eta, mu, sigma, Laves, etc., resulting in variation of alloy properties.

### 1.1. Precipitation Hardening [7-10]

Precipitation hardening [7] is produced by solution treating and quenching an alloy in which a second phase is in solid solution at the elevated temperature but precipitates on quenching and ageing at a lower temperature. Thus, an element can participate in formation of intermetallic precipitates during precipitation strengthening only if it is partially soluble in the matrix. Among all other theories, Coherent Lattice theory is one of the most useful theories for the understanding of precipitation hardening. In precipitation hardening, the alloy is first solutionized by heating into a single phase region and soaking for sufficient time in order to allow the intermetallic and grain boundary precipitates to dissolve in the matrix and also to permit required diffusion. After solution treatment, the alloy is rapid quenched to get a supersaturated solid solution and to prevent formation of equilibrium precipitates due to natural ageing. In supersaturated solid solution (SSS), the alloy is in disordered condition as the solute atoms are at-random distributed in the lattice structure. The alloy during reheating to slightly higher temperature undergoes artificial ageing. Artificial ageing results in limited mobility of soluble atoms and the atoms can move over only a few interatomic distances leading to formation of a fine scale transition structure. Due to slow cooling, rearrangement of the atoms takes place, where the solute atoms move into definite positions in the lattice, forming an ordered solid solution. The ordered transitional structure thus formed will have definite lattice parameters different from the solute atoms will result in coherency of the atom. There will be considerable distortion of the matrix due to fine precipitates thus formed within the matrix and this distortion extends over a large volume only if the excess transition phase is in the form of fine discrete particles well distributed in the matrix. These fine precipitates will restrict the dislocation movement, resulting in rapid increase of strength and hardness of

the alloy during ageing. Eventually, equilibrium-stable phase is formed from the transition phase, whose particles have common grain boundaries of the matrix and there is further growth of certain larger particles at the expense of neighboring smaller particles. This causes loss of coherency with the matrix and stress relief takes place in the lattice, which results in considerable decrease in strength and increase in ductility of the alloy. At this stage, the alloy is said to be overaged. The following steps [10] are associated with the process of precipitation hardening:

1. Rearrangement of atoms within the crystal structure during which micro-strains in the lattice are developed and mechanical properties are improved.
2. Optimum strengthening of the alloy by forming intermediate phase.
3. And finally, formation of stable phase from the transition phase, resulting in decrease of hardness and strength.

It is necessary to understand the above-mentioned three main steps of precipitation hardening, in order to age the alloy to optimum level for considerable increase in strength and hardness. Thus, the degree of strengthening resulting from the secondary phase particles depends on distribution of the particles in matrix.

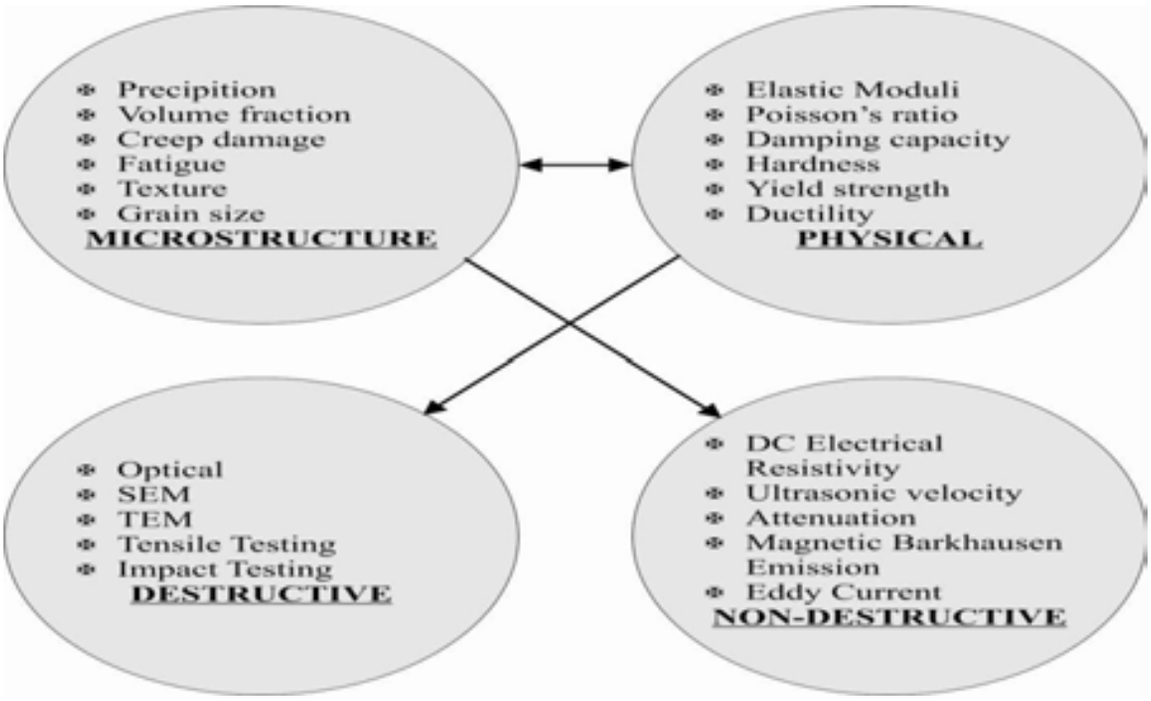


**Figure 1.** Correlation between microstructure, physical and mechanical properties of the material

### 1.2. Non-destructive techniques

Non-destructive Testing (NDT) techniques [11-14] are most commonly used for detection and characterization of flaws in the component, thus certifying whether the component is fit for

http://dx.doi.org/10.5772/61119

the intended service or not. As crystallographic texture controls the plastic and elastic properties of the component, component material property is equally important to assess the structural integrity of the component along with the flaw characteristics. Improved instrumentation and a quantitative understanding of the materials behavior has driven the upgrowth of Quantitative Non-destructive Evaluation (NDE) to detect and characterize microstructural properties as well as flaws in materials. Two quantitative NDE approaches are now in use – 'off-line' periodic inspection during scheduled outages and 'on-line' monitoring [15, 16] during service as well as during materials processing – in order to predict future performance and reliability of components by controlling materials behavior (especially the mechanical properties) with the help of physical mechanisms. Thus, there is correlation between the microstructure of the material with its physical and mechanical properties (Fig. 1) and as these properties can be easily measured by NDE techniques, NDE can be used as a non-destructive tool at low and affordable cost for non-intrusive investigation of the component at regular intervals of the process stages by evaluating the microstructures for many critical applications. During the development of NDE, it was realized that a wide range of techniques are necessary to achieve some flexibility in non-destructive characterization and evaluation of structural materials and components with complex shapes. The present study is mainly devoted to the application of DC electrical resistivity and Ultrasonic NDE techniques to materials characterization.

### 1.3. Non-destructive evaluation

Non-destructive testing (NDT), Non-destructive evaluation [17-32] (NDE) and Non-destructive inspection (NDI) are the techniques that are based [33-43] on the application of determining the characteristics of materials or components and for assessing life of the component by evaluating the detected inhomogeneities and harmful defects present in the component without impairing its usefulness. During service, many factors [17] like unanticipated stresses (residual and system), operation outside designed limits (excessive temperature and load cycling), operation and environmental effects, degradation of material properties in service, etc., which are difficult to predict, affect the designed life of the component. It may not be possible to take a sample from the component and determine its health for continued service. Moreover, efforts to increase the lifetime of intricate and expensive structures like aircraft, space shuttle engine and gas turbine require on-line monitoring of the microstructure in order to improve the safety and maintainability by analyzing the current state of the component. Thus, NDE techniques used for characterization [17, 24, 25] of the material properties are of great significance during service life of the component as they help in controlling process parameters by providing timely feedback.

#### *1.3.1. Advantages of NDT over destructive testing*

- In-service testing is possible.
- Tests are made directly on the component itself and thus special coupon of the component is not required.

- Very little sample preparation of the test specimen is required.
- Less time requirement for testing.
- Repeated checks over a period of time are possible.
- A single NDT can measure many or sometimes all properties of the alloy.
- Some NDT instruments are portable and can be easily carried to the workplace.

*1.3.2. Limitations of NDT*

- Measurements are indirect and hence reliability has to be verified.
- Some of the NDT techniques are expensive.
- Skilled judgement and experience are required to interpret NDT results.

*1.3.3. Examples of case studies carried out for assessment of components with the help of NDT*

**1.** Characterization of microstructural and mechanical properties:

- Measurement of grain size [17, 44-47] with the help of ultrasonic testing.
- Microstructural control in [18] Metal Matrix Composites (MMC).
- Estimation of non-metallic inclusions [17] in steel. There is an ASTM standard E 588 titled 'Detection of large inclusions in bearing quality steel by ultrasonic method'. Also porosity [18] can be characterized.
- Measurement of degree of recrystallization [48].
- Determination of elastic modulus [49] especially for brittle materials since other methods like tensile test, do not produce optimum results.
- Estimation of strength [50].
- Ultrasonic hardness [17] testers are also used especially for in situ measurements.
- For monitoring [51] ductile to brittle transition temperature (DBTT).
- Fracture toughness [52] can be estimated using ultrasonic testing as Kc (fracture toughness) is dependent on the value of E (Young's Modulus) by the equation ($Kc = \sqrt{E} * Gc$). Kc depends upon the ultrasonic attenuation while E can be calculated using ultrasonic velocity.

**2.** For qualification of processing techniques like the following:

**1.** Nodularity of cast iron, as the increase in degree of nodularity (morphology of graphite) increases the strength, which in turn increases ultrasonic velocity [53,54].

**2.** Qualification of heat treatment of precipitation hardenable 17-4 PH stainless steel [55] using ultrasonic testing.

http://dx.doi.org/10.5772/61119

rmination of elastic modulus [49] especially for brittle materials since other methods like
nsile test, do not produce optimum results.
mation of strength [50].
rasonic hardness [17] testers are also used especially for in situ measurements.
monitoring [51] ductile to brittle transition temperature (DBTT).
cture toughness [52] can be estimated using ultrasonic testing as Kc (fracture toughness) is
pendent on the value of E (Young's Modulus) by the equation (Kc = √E * Gc). Kc
epends upon the ultrasonic attenuation while E can be calculated using ultrasonic velocity.
ification of processing techniques like the following:
dularity of cast iron, as the increase in degree of nodularity (morphology of graphite)
creases the strength, which in turn increases ultrasonic velocity [53,54].
alification of heat treatment of precipitation hardenable 17-4 PH stainless steel [55] using
trasonic testing.
curate measurement of case depth [56] in order to have knowledge about component's
ardness.
asuring degree of diffusion bonding [57-59].
et metal formability [60].
erization of material degradation during in-service:
ection of fatigue [61, 62] and creep [63] failure in turbine blade made of Superalloy.
ection of hydrogen attack in low alloy steel [64, 65] and in Zircaloy-2.
rgranular corrosion attack in austenitic stainless steel [66].
rmal embrittlement [67] of Duplex stainless steel.
eing degradation in Ni-based Superalloy 625 [49,68].
essment of degradation of a heavy water plant [12].
ure of S.S dished ends during storage with the help of in situ metallography at the inner
rface of the failed dished end [12].

**electrical resistivity**

cal resistivity is one of the oldest non-
electromagnetic techniques. The electrical
of a material depends on its physical state
emperature and stress along with its
n and microstructure. The congential
e of the resistivity on the microstructure

3. Accurate measurement of case depth [56] in order to have knowledge about component's hardness.
4. Measuring degree of diffusion bonding [57-59].
5. Sheet metal formability [60].

3. Characterization of material degradation during in-service:
of case depth [56] in order to have knowledge about component's
- Detection of fatigue [61, 62] and creep [63] failure in turbine blade made of Superalloy.
- Detection of hydrogen attack in low alloy steel [64, 65] and in Zircaloy-2.
- Intergranular corrosion attack in austenitic stainless steel [66].
- Thermal embrittlement [67] of Duplex stainless steel.
- Ageing degradation in Ni-based Superalloy 625 [49,68].
- Assessment of degradation of a heavy water plant [12].
- Failure of S.S dished ends during storage with the help of in situ metallography at the inner surface of the failed dished end [12].

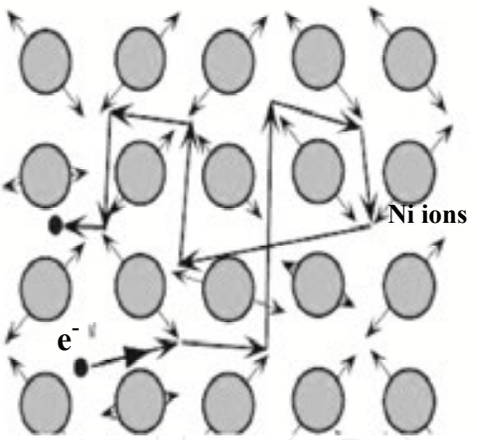


Figure 2. Random motion of electron due to thermal vibrations[71]

**Figure 2.** Random motion of electron due to thermal vibrations

### 1.4. DC electrical resistivity

DC electrical resistivity is one of the oldest non-destructive electromagnetic techniques. The electrical resisitivity of a material depends on its physical state such as temperature and stress along with its composition and microstructure. The congential dependence of the resistivity on the microstructure can be helpful to detect various transformations in the material due to thermal exposure. Measuring material's resistivity non-destructively helps in identifying various metals and alloys and monitoring the heat treatment of the alloy; along with the detection of damage that gives rise to a change in resistivity [11,69]. The precipitation hardening has been believed [70] to arise from the formation of very small solute clusters which uses significant scattering of the conduction electron (Fig. 2) [71] and hence the electrical

resistivity of the aged alloy increases. In the absence of an applied field, there is no net drift in any direction and conduction electron in the metal moves about randomly scattered (with a mean speed) by thermal vibrations of the atoms. Resistivity, in short, varies as a result of combined effects [72,73] from solution depletion, intermetallic precipitates, high-temperature solute enrichment due to the dissolution of the clusters formed during ageing and also refining of the intermetallic precipitates. Four-point direct current potential drop (DCPD) technique [69] is well suited for accurate non-destructive measurement of material resistivity. The potential drop method of evaluation is based on the principle that the electrical resistance of an alloy changes due to the presence of structural inhomogeneities. Thus, measuring bulk resistivity using DCPD one can have knowledge about performance and reliability of the component. Direct current potential drop (DCPD) technique is independent of the magnetic permeability of the material and is also useful for testing ferrous as well as low-conductivity materials. Moreover, DCPD equipment is simpler and requires less controlled parameters and there is possibility of full automation of the monitoring.

### 1.5. Ultrasonic testing

Ultrasonic Testing is the most preferred NDE technique for material property characterization, as UT parameters are significantly affected by changes in microstructure or mechanical properties of the material. Microstructural properties [17] like grain size measurement [44-47]; estimating presence of inclusions; measuring degree of recrystallization [48]; mechanical properties like elastic modulus, hardness [13], fracture toughness [52], and estimating strength [50] of the structure; monitoring of Ductile Brittle Transition Temperature [51] (DBTT) are correlated with ultrasonic testing parameters which include variation in the frequency and velocity [74], attenuation [52], backscatter amplitude [44], spectral analysis and acoustic microscopy. Ultrasonic material characterization has also been used to qualify various processing treatments like precipitation hardening, case hardening along with the assess of damage due to various degradation mechanisms [61-68] like fatigue, creep, corrosion, hydrogen damage, thermal embrittlement of steel, ageing degradation, etc. Elastic properties of the component can be easily recognized by the measurements of the Young's Modulus with the help of ultrasonic wave speed and attenuation measurements. Elastic moduli of pure metal are very low which will further increase with the addition of the alloying elements and during precipitation hardening. Ultrasonic velocity will be influenced [18] by the elastic moduli of the material which will be influenced by the precipitate forming elements. Information about microstructural induced changes in the elastic moduli can be deduced from the ultrasonic velocity by Equation 1:

$$v = \sqrt{c/\rho} \tag{1}$$

where $v$= ultrasonic velocity, $c$= elastic stiffness and $\rho$= density.

Ultrasonic velocity (v) measurement involves determination of the distance travelled by the ultrasound and dividing it by time of travel between the first and second back surface echo, as mentioned in Equation 2:

http://dx.doi.org/10.5772/61119

$$v = 2h/t \tag{2}$$

where, $v$ = ultrasonic velocity, $h$ = sample thickness and $t$ = time of flight.

The accuracy of these measurements depends upon the accuracy with which time of flight and thickness of the component are measured. With advancement [75-78] and use of software (e.g. LabVIEW, MATLAB), one can calculate ultrasonic velocity with accuracy of 500 μsec, making it a very reliable parameter for material property characterization.

## 2. Research undertaken

A study is carried out to characterize different microstructural features and the precipitation behaviour evolved through various heat treatments using Direct Current Potential Drop (DCPD) technique for measuring electrical resistivity and Ultrasonic Testing for measurements of ultrasonic parameters and validating the same with hardness and microstructural features. Table 1 and Table 2 show the chemical composition of Ni-263 and IN- 718 superalloys under study.

| **Element** | C | Co | Cr | Mo | Ti | Al | Cu | O | N | Ni |
|---|---|---|---|---|---|---|---|---|---|---|
| **wt%** | 0.06 | 19.60 | 20.1 | 6.00 | 2.00 | 0.4 | 0.001 | 0.0013 | 0.006 | Bal |

**Table 1.** Chemical composition of Nimonic 263

| **Element** | Ni | Fe | Cr | Ti | Al | Nb | Mo | Co | C | Mn |
|---|---|---|---|---|---|---|---|---|---|---|
| **wt%** | 53.30 | 17.66 | 19.21 | 1.03 | 0.4 | 5.06 | 2.92 | 0.01 | 0.04 | <0.10 |

**Table 2.** Chemical composition of Inconel 718

### 2.1. Heat treatment cycle

| **Temperature** | **Time (h)** | **Expected Phase** |
|---|---|---|
| **SA + 650(C + 620(C (8 h)** | 10, 25, 50, 75, 100 | γ |
| **SA + 750(C + 620(C (8 h)** | 10, 25, 50, 75 | γ′ + γ″ |
| **SA + 800(C + 620(C (8 h)** | 25, 50, 75 | γ′+ γ″ + δ |
| **SA + 900(C** | 75, 100 | δ |

**Table 3.** Test matrix for IN-718 specimens

A set of Ni-263 specimens of dimensions 20 mm×20 mm×10 mm was solution annealed (SA) at 1150ºC for 1 h followed by water quenching. Referring to the TTT diagram of Ni-263 [79], the SA specimens were thermally aged for 1, 2, 4, 6 and 8 h at 650ºC and 1, 2, 4, 6, 25, 50 and 75 h at 800ºC, followed by water quenching. Similarly, a set of IN-718 specimens of dimensions 25mm x 29mm x 10mm was subjected to solution annealing at 980ºC for 1 hr and then water quenched to room temperature. Further solution annealed (SA) IN-718 specimens were aged by giving two-step ageing treatment, thereby forming new intermetallic precipitates and various phases depending on the time and temperature of ageing. Referring to the TTT diagram of IN-718 [2,80], test matrix was designed for the specimens in such a way that all the specimens have varying microstructures with difference in size and percentage of intermetallic precipitates. Figure 4 shows the experimental temperature for IN-718 in TTT diagram and Table 3 shows the test matrix for IN-718 with various expected phases.

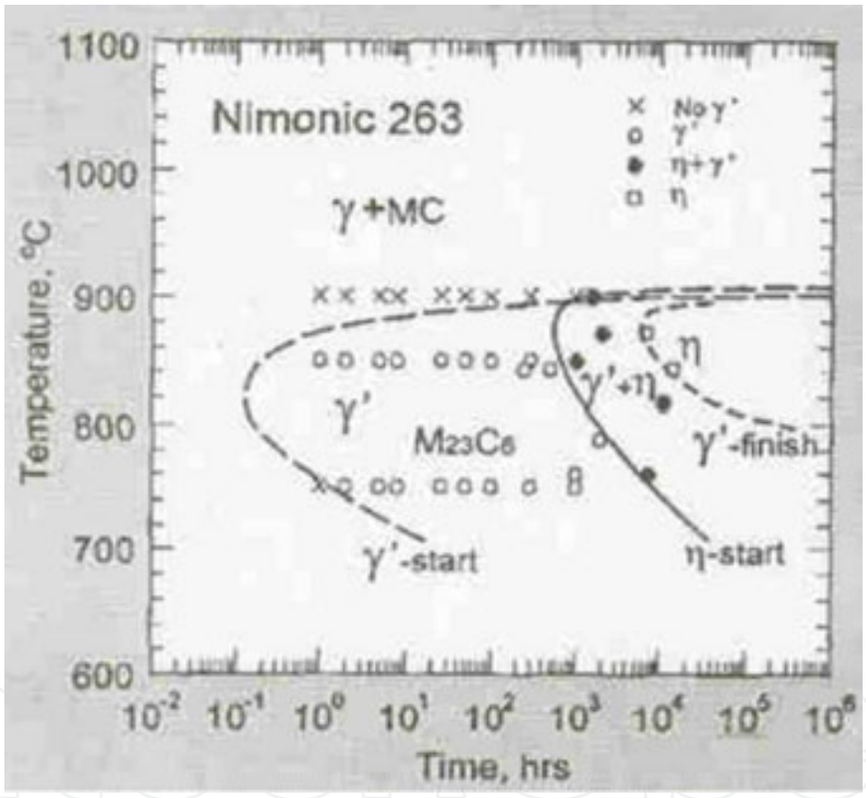


**Figure 3.** TTT diagram of Ni-263

### 2.2. Resistivity measurement

For resistivity measurement, four-probe Van der Pauw method has been used. In this method, electrical DC currents are injected into a conducting specimen through a set of two probes; while a second set of two probes is used for measuring the voltage drop across the area of contact as shown in Fig. 5. After an accurate measurement of the distance between the voltage probes, the resistivity (ϱ) of the sample is measured using Equation 3:

http://dx.doi.org/10.5772/61119

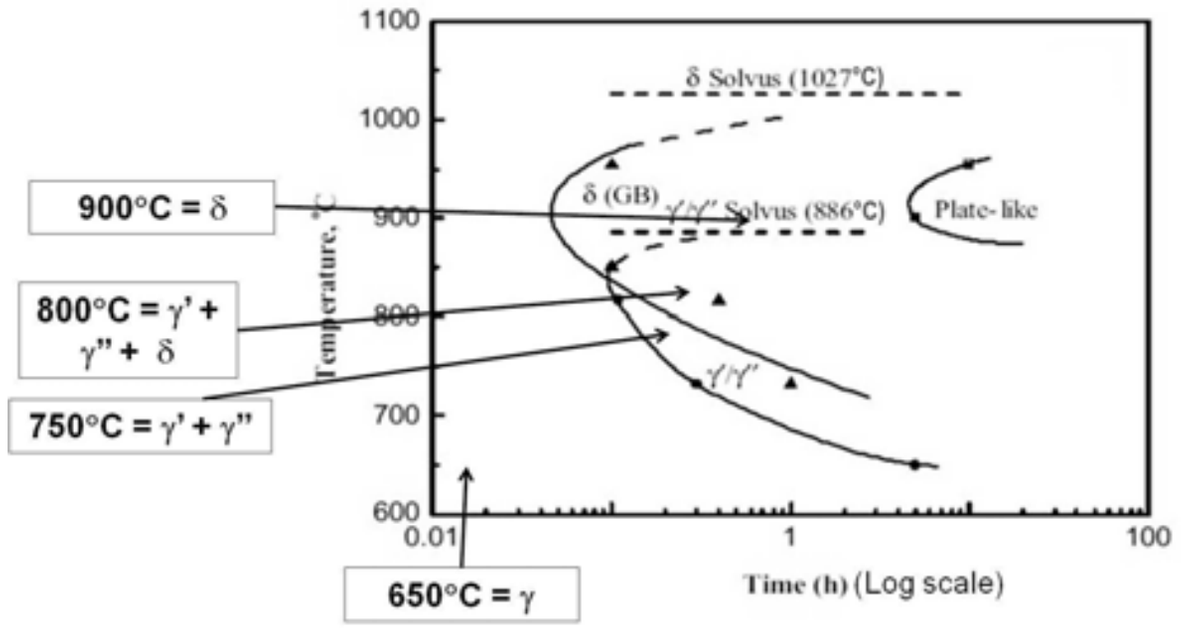


**Figure 4.** TTT diagram of IN-718 with experimental temperature

$$\rho = RA/L \tag{3}$$

where R = resistance or voltage drop when a constant current is passed.

A = cross-sectional area of contact of the sample.

L = distance between the voltage probes.

For better accuracy and speed of measurement, a sample holder has been used; in which four contacts are made by pressure contacts with gold tips. Keithley 2400 Sourcemeter is used as constant current source; while Keithley 2182A Voltmeter is used for measurement of the voltage drop. Resistivity for all the specimens was calculated with 0.03% error. Error percentage was determined using the maximum variation in the average resistivity value for each specimen.

### 2.3. Ultrasonic velocity measurements

The experimental set-up used for Ultrasonic Velocity (UV) measurement is shown in Fig. 6. A broadband pulser-receiver and a 500 MHz digital oscilloscope were used for carrying out the ultrasonic measurements. For UV measurements, the RF signals were digitized and stored for further processing. Ultrasonic velocities were measured using 5 MHz longitudinal wave transducer. For better accuracy and speed of measurement, a software is used for calculating ultrasonic velocity and attenuation of the sample by reading the digitized RF signals and the gated back wall echo from the oscilloscope stored in the computer. The accuracy obtained in the time of flight measurement is improved by 500 μsec, which led to maximum scattering of ±3m/s for ultrasonic longitudinal velocity.

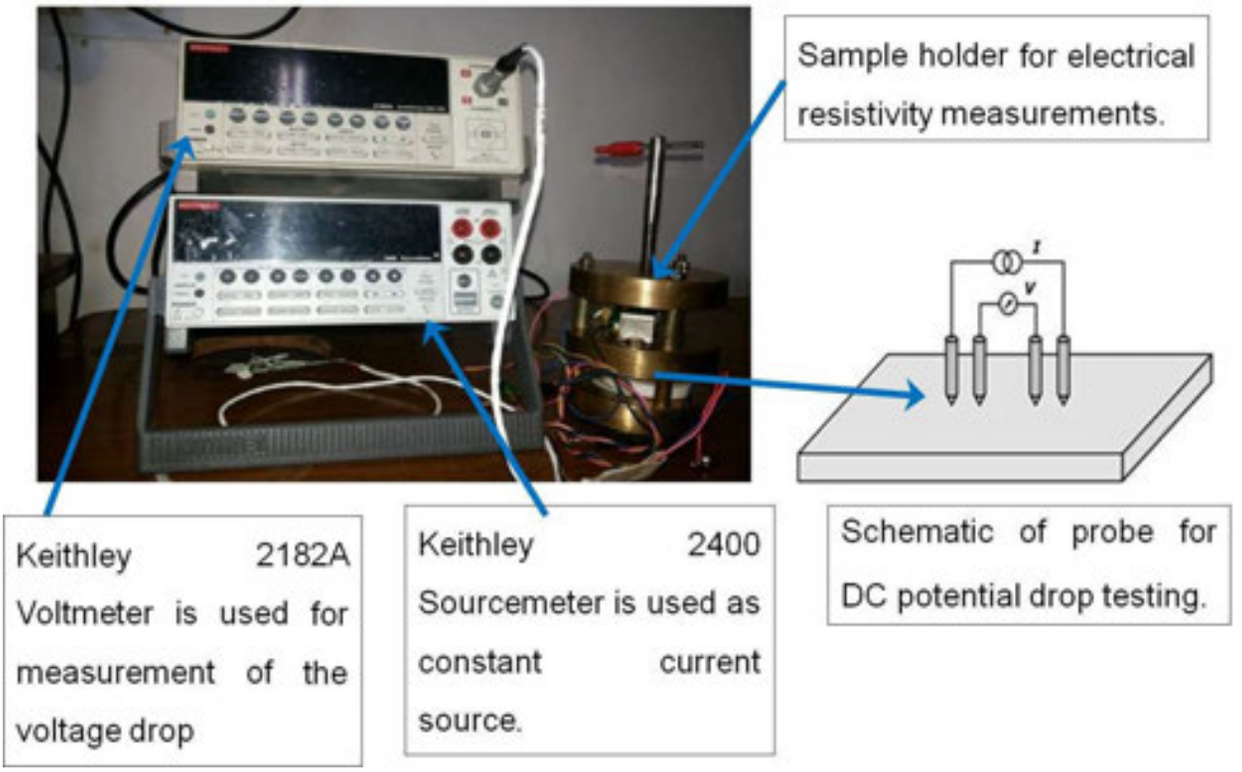


**Figure 5.** DC Electrical resistivity measurement set-up

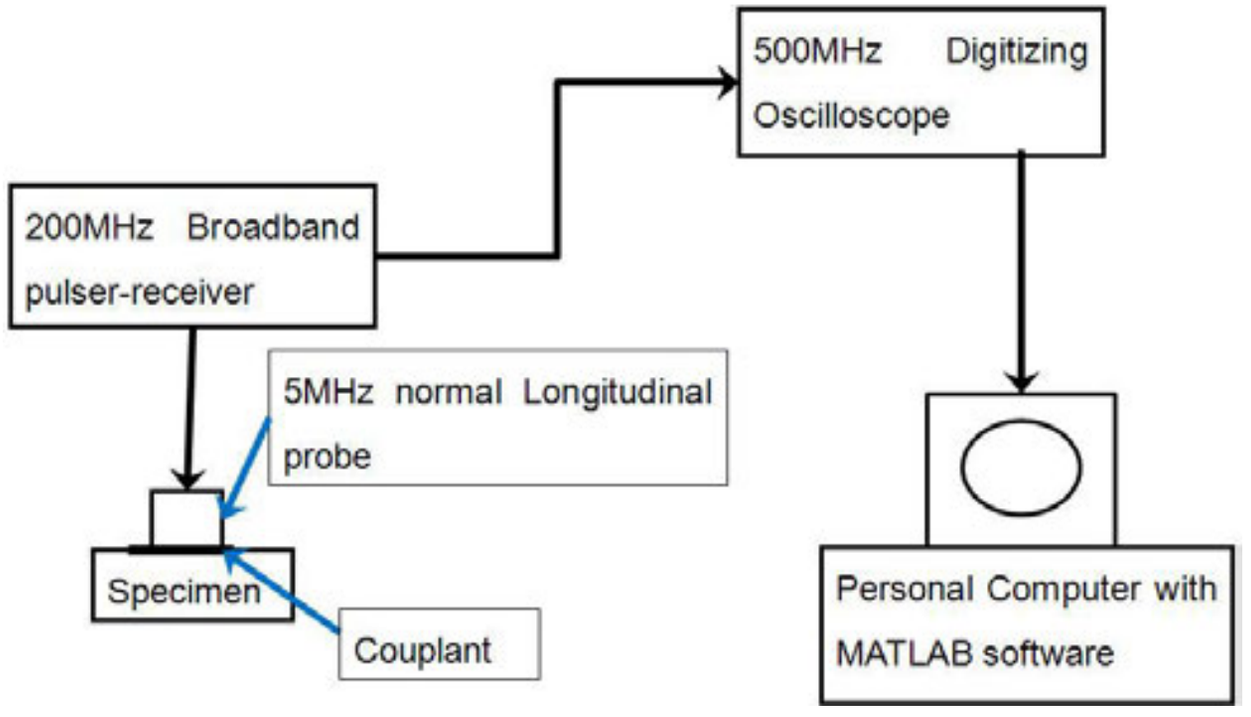


**Figure 6.** Ultrasonic velocity measurement set-up

http://dx.doi.org/10.5772/61119

### 2.4. Hardness measurements

Hardness measurements were carried out using Indentation method by applying a load of 700 N. A maximum change of ±5 BHN is obtained in hardness measurements in any specimen. Image analysis and Scanning Electron Microscopy were carried out to study the precipitation behaviour, and validate the results.

## 3. Observations

### 3.1. Resistivity observations

Table 4 and Table 5 show the variation in the resistivity with different ageing cycles. An average of 8 readings is taken as final resistance value. Resistivity measures the difficulty of electrons to move freely in the alloy. Additional ageing will lead to the formation of ordered clusters and precipitates, which will result in significant scattering of conducting electrons as they vibrate around equilibrium positions. A key factor for electron scattering is the lattice vibrations. As an electron encounters a defect in form of fine precipitates or due to the presence of other inhomogeneities, it scatters from its path by losing energy and changing direction.

Based on the experimental work, it is observed that resistivity of solution annealed specimen is the highest which will be further affected by the cluster formation; which is again dependent on the ageing time and temperature. During precipitation, the initial nucleation of the fine precipitate phase results in a maximum increase of resistivity due to the decreased conduction electron mean free path associated with forming these scattering electrons within the matrix phase. As the precipitates undergo growth and coarsening on increase of ageing temperature and time, the dispersed fine precipitate phase converts to a more widely spaced phase. Conduction electrons are now more likely to collide with solute atoms than the coarse precipitates. After a maximum, the resistivity thus begins to decrease due to the growth and coarsening of the precipitates and also due to the changes to the solute content from the increasing precipitate volume fraction. Thus, resistivity is not only dependent on kinetics of precipitation but is also affected by scattering of electrons. Resistivity, in short, varies as a result of combined effects from solution depletion, intermetallic precipitates, high-temperature solute enrichment due to the dissolution of the clusters formed during ageing and also refining of the intermetallic precipitates. These changes in resistivity at higher temperature will also be there due to the presence of pre-existing intermetallic precipitates, as they affect the rate of electron scattering and also by forming coarse grain structure which will slow down the kinetics of the precipitation by reducing nucleation rate. At lower temperature, due to increase in precipitate to the equilibrium volume fraction, the resistivity shows similar peak positions in the maximum increased resistivity. Bulk resistivity decreases on increase of ordering of the material.

### 3.2. Ultrasonic velocity observations

It is observed from Table 4 and Table 5 that ultrasonic velocity is influenced by the volume fraction, coherency, fineness and distribution of the precipitates. Longitudinal wave velocity

is found to increase with ageing time and temperature. The increase in velocity with ageing time is found to be maximum at initial stages (indicating possible faster kinetics). Elastic moduli of pure metal are very low which will further increase with the addition of the alloying elements and this will also affect ultrasonic velocity of the material. During incubation period, there will be influence of the precipitate forming elements on the elastic moduli of the alloy. Formation of intermediate coherent transition γ″- phase in alloy will drastically affect the elastic moduli of the alloy, resulting in increase of ultrasonic velocity of the alloy. The inter-metallic precipitates so formed lead to an increase in the elastic moduli of the alloy and consequently increases the ultrasonic velocities in Superalloys [49 and references therein]. However, the ageing of the alloy if carried out for shorter durations at any temperature leads to decrease in the ultrasonic velocity due to the dissolution of the intermetallic precipitates. Further, the formation of stable orthorhombic δ-phase by coarsening of γ″- precipitates increases the ultrasonic velocity. The increase in the moduli upon thermal ageing is attributed to the formation of γ′ and γ″-precipitates leading to the depletion of the precipitate forming elements like Nb, Al and Ti from the solution. Again it is observed that ultrasonic velocity is only affected by the intermetallic precipitates and not by the grain-boundary carbides. Thus, ultrasonic velocity is sensitive to initial nucleation of the precipitates along with their growth and coarsening. The depletion of the precipitate-forming elements from the matrix during coarsening leads to an increase in the modulus of the matrix.

### 3.3. Hardness

The variations in the hardness, resistivity and ultrasonic velocity with different ageing cycles is shown in Table 4 and Table 5. For Ni-263, the solution annealed specimen exhibited lowest hardness (180 BHN) and it increases with an increase in ageing temperature from 650ºC to 800ºC. On ageing at 650°C, hardness is found to continuously increase with increase in time of exposure (2 h, 4 h, 6 h, 8 h, 25 h, 50 h, 75 h and 100 h). The strength of the specimen will decrease due to overageing of the specimen at higher temperature resulting in coarsening of grains. While on ageing at 800°C hardness initially increases with time of exposure but decreases for longer ageing time. This is in agreement with the expected phase diagram. The increase in strength by ageing is due to the presence of fine and uniformly distributed metastable coherent γ′ precipitates in the matrix. While at higher temperature above 800°C there is decrease in the strength due to overageing, resulting in rapid coarsening of fine coherent γ′ phase and its conversion to accicular η-phase. η-phase degrades the strength of the alloy by consuming the solution strengthening elements and this is one of the reasons for decrease in hardness at 800°C for longer exposure time. The results obtained are in line with the time temperature transformation (TTT) diagram reported in literature for the precipitation of γ′ intermetallic phase in this alloy and further confirmed by microscopy studies.

Similarly for IN-718, the SA specimen exhibited lowest hardness (165 BHN) and it increases with an increase in ageing temperature from 600°C to 750°C. But there is a decrease in hardness on further increase of temperature from 750°C to 900°C. On ageing at 650°C, hardness is found to continuously increase with increase in time of exposure (10 h, 25 h, 50 h, 75 h and 100 h). The strength of the specimen will decrease due to overageing of the specimen at higher

http://dx.doi.org/10.5772/61119

temperature, resulting in coarsening of grains. While on ageing at 750°C and 800°C, hardness initially increases with time of exposure but decreases for longer ageing time. Again on ageing at 750°C, hardness is initially found to increase with increase in time of exposure and further exposure decreases the hardness values. On the other hand, for ageing at 900°C it decreases continuously. This is in agreement with the expected phase diagram. The increase in strength by ageing is due to the presence of fine and uniformly distributed metastable phase γ″ in the matrix. While at higher temperature above 750°C there is decrease in the strength due to overageing, resulting in rapid coarsening of γ″. At 800°C, it is expected from the TTT diagram that for longer time of exposure, nucleation of stable orthorhombic δ-phase will start from γ″. δ-phase degrades the strength of the alloy by consuming the precipitation strengthening elements. And this is one of the reasons for decrease in hardness at 800°C and 900°C for longer exposure time. During overageing hardness will reduce to lower values. Along with the formation of delta (δ) phase at the higher temperature, there will also be the formation of MC-type grain boundary carbides, which will also affect the hardness of the alloy. The variation in hardness with ageing time and temperature is also confirmed by electron microscopy studies.

| Ageing Cycle | Ultrasonic Velocity (m/s) | Resistivity | Hardness [BHN] |
|---|---|---|---|
| **1150ºC for 1 h (SA)** | 5960 | 131.60 | 180.40 |
| **SA+650ºC / 2 h** | 5980 | 137.70 | 216.10 |
| **SA+650ºC / 4 h** | 5992 | 142.97 | 228.43 |
| **SA+650ºC / 6 h** | 5993 | 147.97 | 231.20 |
| **SA+650ºC / 8 h** | 5995 | 143.77 | 244.83 |
| **SA+650ºC / 25 h** | | 140.72 | 247.60 |
| **SA+650ºC / 50 h** | | 140.46 | 265.43 |
| **SA+650ºC / 75 h** | | 138.78 | 276.70 |
| **SA+650ºC / 100 h** | | 136.43 | 281.90 |
| **SA+800ºC / 2 h** | 5982 | 139.21 | 246.60 |
| **SA+800ºC / 4 h** | 5987 | 139.37 | 270.70 |
| **SA+800ºC / 6 h** | 5988 | 136.87 | 278.53 |
| **SA+800ºC / 8 h** | | 141.40 | 280.17 |
| **SA+800ºC / 25 h** | 5987 | 136.10 | 293.77 |
| **SA+800ºC / 50 h** | 5986 | 137.33 | 307.50 |
| **SA+800ºC / 75 h** | 5985 | 139.00 | 310.53 |
| **SA+800ºC / 100 h** | | 136.37 | 303.57 |

**Table 4.** Ultrasonic Velocity, Resistivity and Hardness of Nimonic 263 in different heat treatment conditions

| Ageing Cycle | Ultrasonic Velocity (m/s) | Resistivity [Ωm] | Hardness [BHN] |
|---|---|---|---|
| **980°C for 1 h (SA)** | 5786 | $1.2467*10^{-6}$ | 165 |
| **SA + 650°C 10 h + 620°C 8 h** | 5800 | $1.2539*10^{-6}$ | 260 |
| **SA + 650°C 25 h + 620°C 8 h** | 5795 | $1.1476*10^{-6}$ | 298 |
| **SA + 650°C 50 h + 620°C 8 h** | 5817 | $1.1236*10^{-6}$ | 328 |
| **SA + 650°C 75 h + 620°C 8 h** | 5815 | $1.0634*10^{-6}$ | 360 |
| **SA + 650°C 100 h + 620°C 8 h** | 5827 | $1.0764*10^{-6}$ | 377 |
| **SA + 750°C 10 h + 620°C 8 h** | 5828 | $1.0462*10^{-6}$ | 385 |
| **SA + 750°C 25 h + 620°C 8 h** | 5813 | $0.9913*10^{-6}$ | 378 |
| **SA + 750°C 50 h + 620°C 8 h** | 5824 | $0.9672*10^{-6}$ | 358 |
| **SA + 750°C 75 h + 620°C 8 h** | 5817 | $1.0131*10^{-6}$ | 349 |
| **SA + 800°C 25 h + 620°C 8 h** | 5836 | $1.0007*10^{-6}$ | 328 |
| **SA + 800°C 50 h + 620°C 8 h** | 5842 | $1.1207*10^{-6}$ | 325 |
| **SA + 800°C 75 h + 620°C 8 h** | 5830 | $1.1139*10^{-6}$ | 309 |
| **SA + 900°C 75 h** | 5843 | $1.1706*10^{-6}$ | 208 |
| **SA + 900°C 100 h** | 5795 | $1.1824*10^{-6}$ | 206 |

**Table 5.** Ultrasonic Velocity, Resistivity and Hardness of IN-718 in different ageing cycles

## 4. Graphs

Figure 7 to Figure 17 are the graphs showing the variations in the hardness, resistivity and ultrasonic velocity with different ageing cycles.

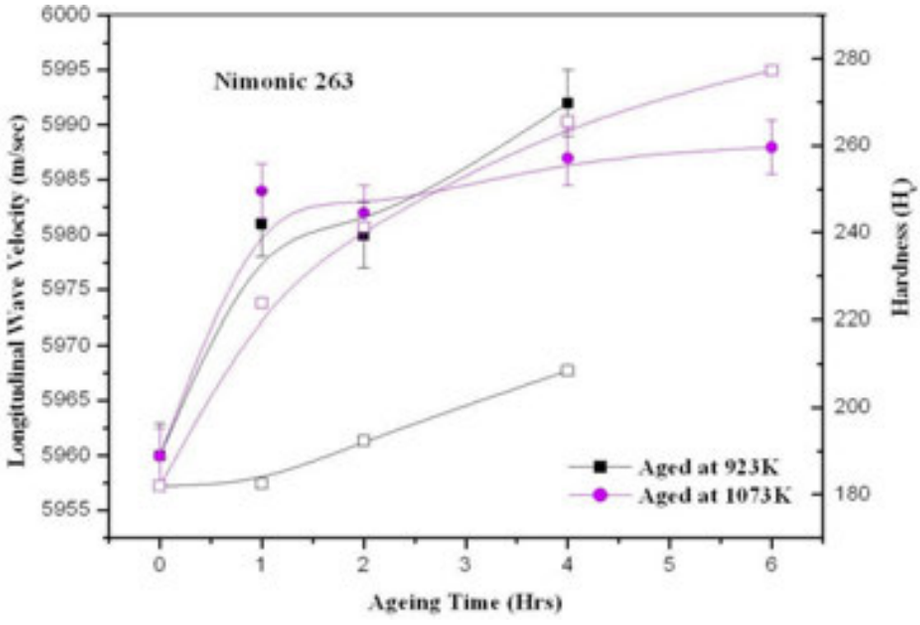


**Figure 7.** Ultrasonic Velocity and Hardness vs. Time for Solution Annealed (SA) specimens thermally aged at 923K (650ºC) and 1023K (800ºC) and studied with respect to the readings of SA specimen

http://dx.doi.org/10.5772/61119

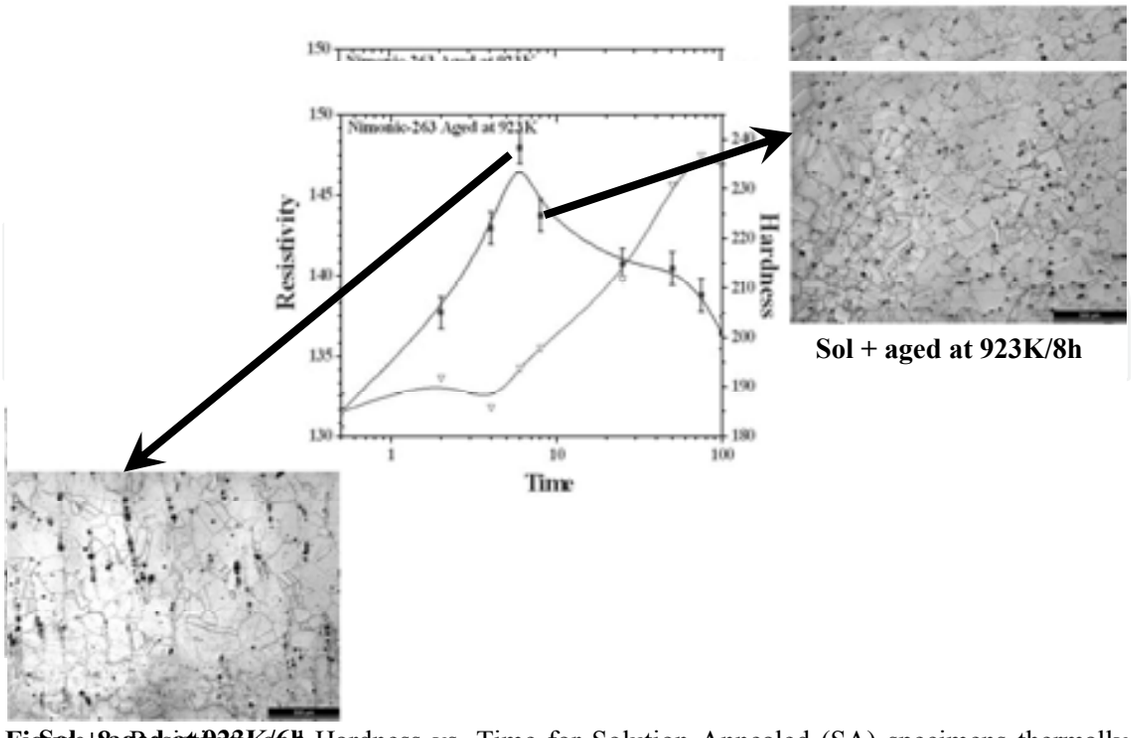


**Figure 8**. Resistivity and Hardness vs. Time for Solution Annealed (SA) specimens thermally aged at 923K (650ºC) and studied with respect to the readings of SA specimen

**Figure 8**. Resistivity and Hardness vs. Time for Solution Annealed (SA) specimens thermally aged at 923K (650ºC) and studied with respect to the readings of SA specimen

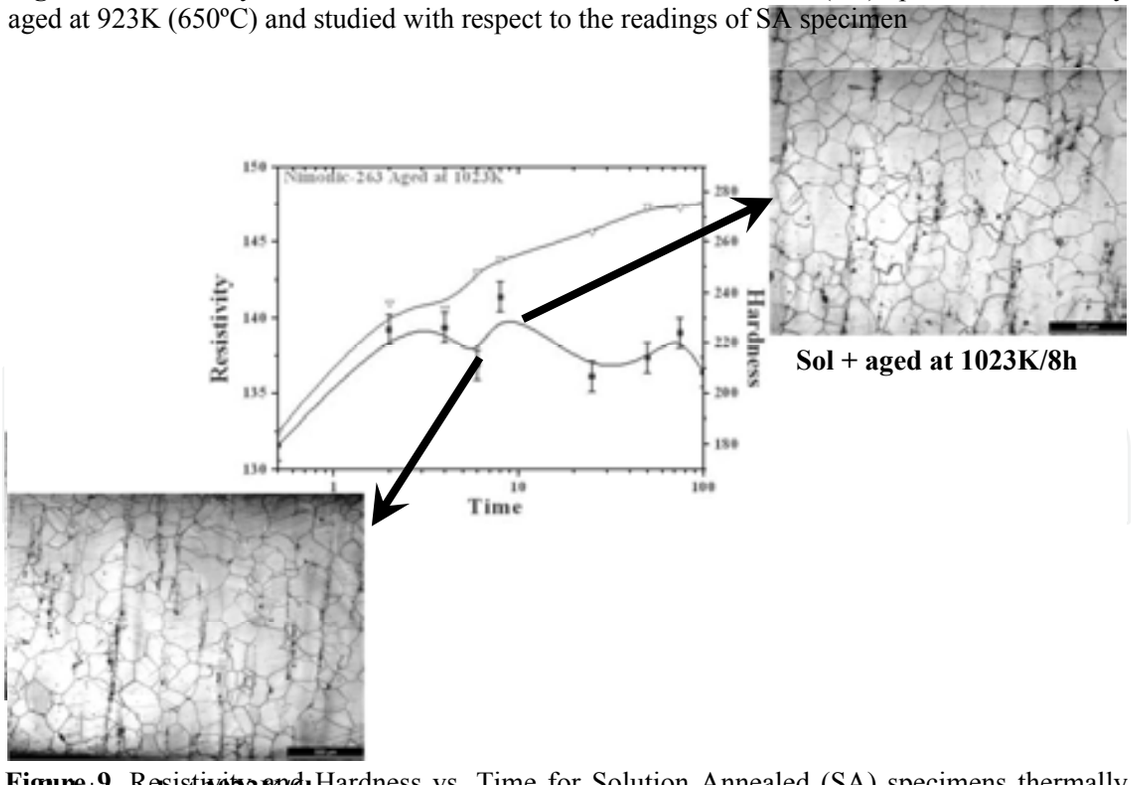


**Figure 9.** Resistivity and Hardness vs. Time for Solution Annealed (SA) specimens thermally aged at 1023K (800ºC) and studied with respect to the readings of SA specimen

**Figure 9.** Resistivity and Hardness vs. Time for Solution Annealed (SA) specimens thermally aged at 1023K (800ºC) and studied with respect to the readings of SA specimen

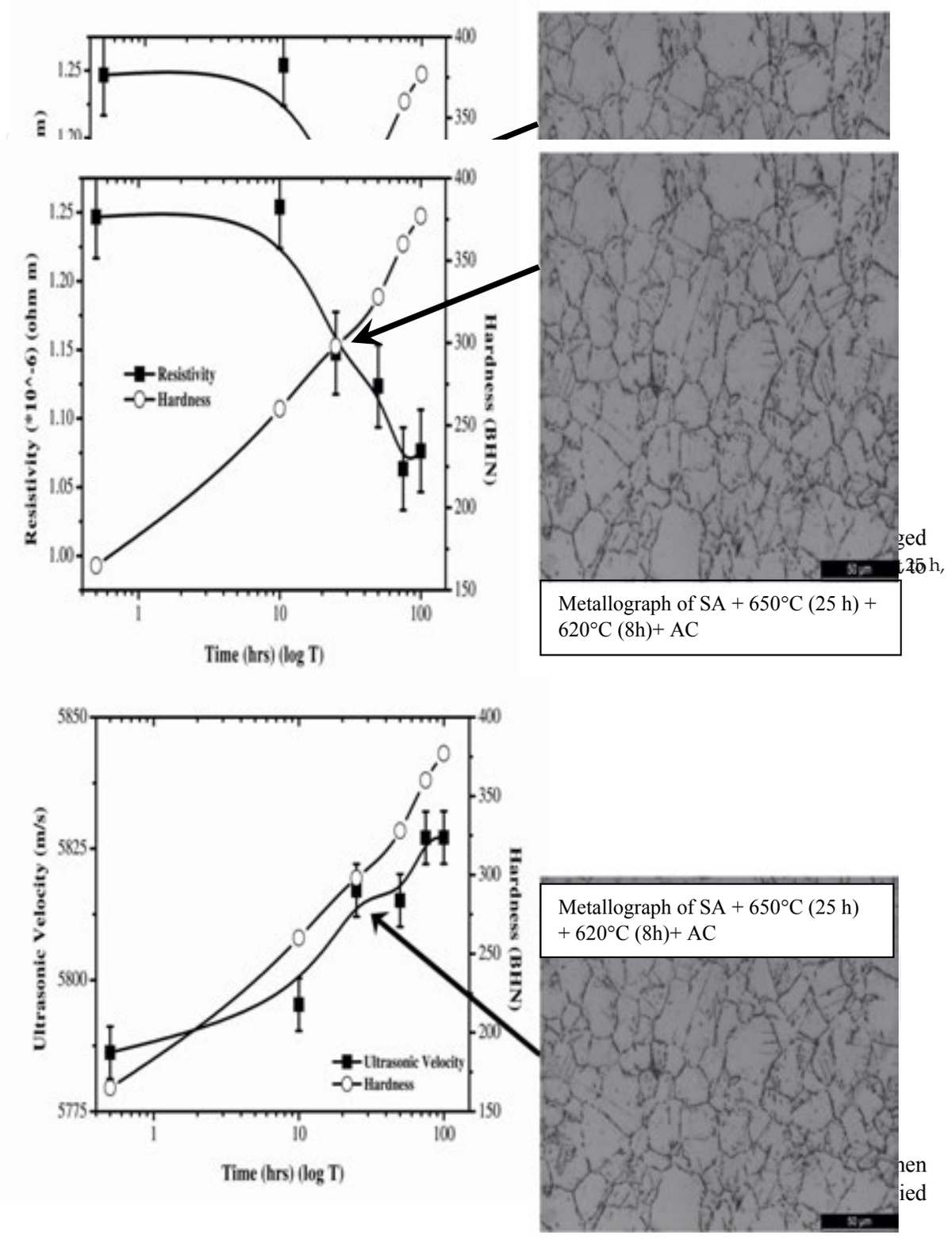


**Figu** ged
50 h, 25 h,
hen
ied

**Figure 11.** Ultrasonic Velocity and Hardness vs. Time for Solution Annealed (SA) specimen thermally aged at 650°C (10 h,25 h,50 h,75 h,100 h) followed by ageing at 620ºC (8 h) and studied with respect to the readings of SA specimen

http://dx.doi.org/10.5772/61119

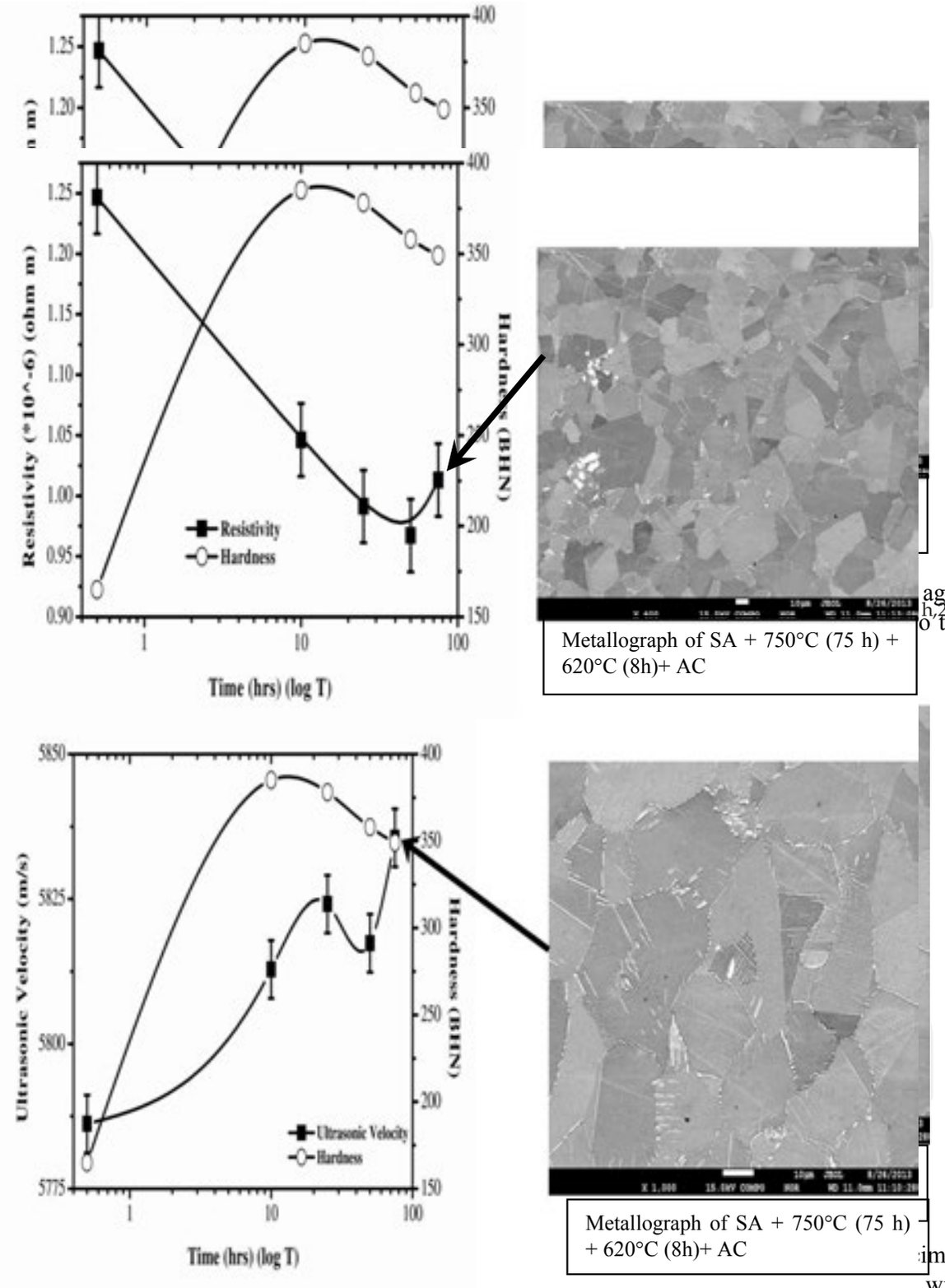


**Figure 13.** Ultrasonic Velocity and Hardness vs. Time for Solution Annealed (SA) specimen thermally aged at 750°C (10 h,25 h, 50 h, 75 h) followed by ageing at 620ºC (8 h) and studied with respect to the readings of SA specimen

**Figure 13.** Ultrasonic Velocity and Hardness vs. Time for Solution Annealed (SA) specimen thermally aged at 750°C (10 h,25 h,50 h,75 h) followed by ageing at 620°C (8 h) and studied with respect to the readings of SA specimen

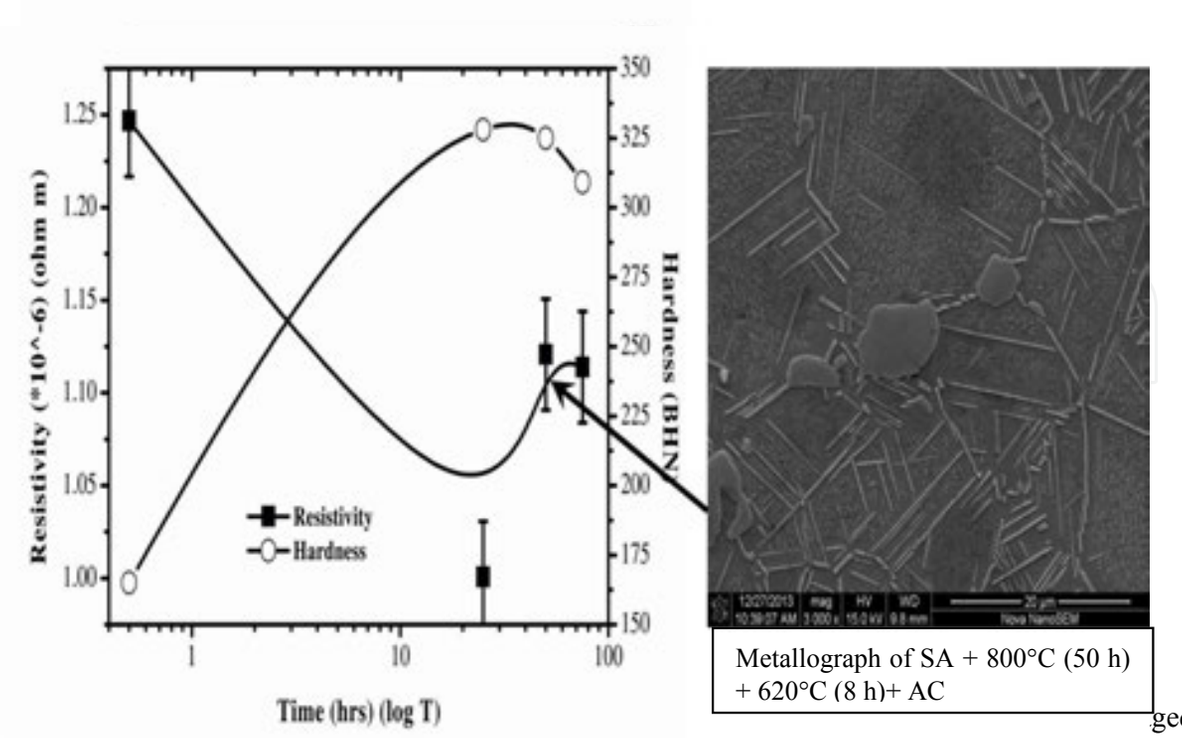


**Figure 14.** Resistivity and Hardness vs. Time for Solution Annealed (SA) specimen thermally aged at 800°C (25 h,50 h,75 h) followed by ageing at 620ºC (8 h) and studied with respect to the readings of SA specimen

Figure 14. Resistivity and Hardness vs. Time for Solution Annealed (SA) specimen thermally aged at 800°C (25 h,50 h, 75 h) followed by ageing at 620°C (8 h) and studied with respect to the readings of SA specimen

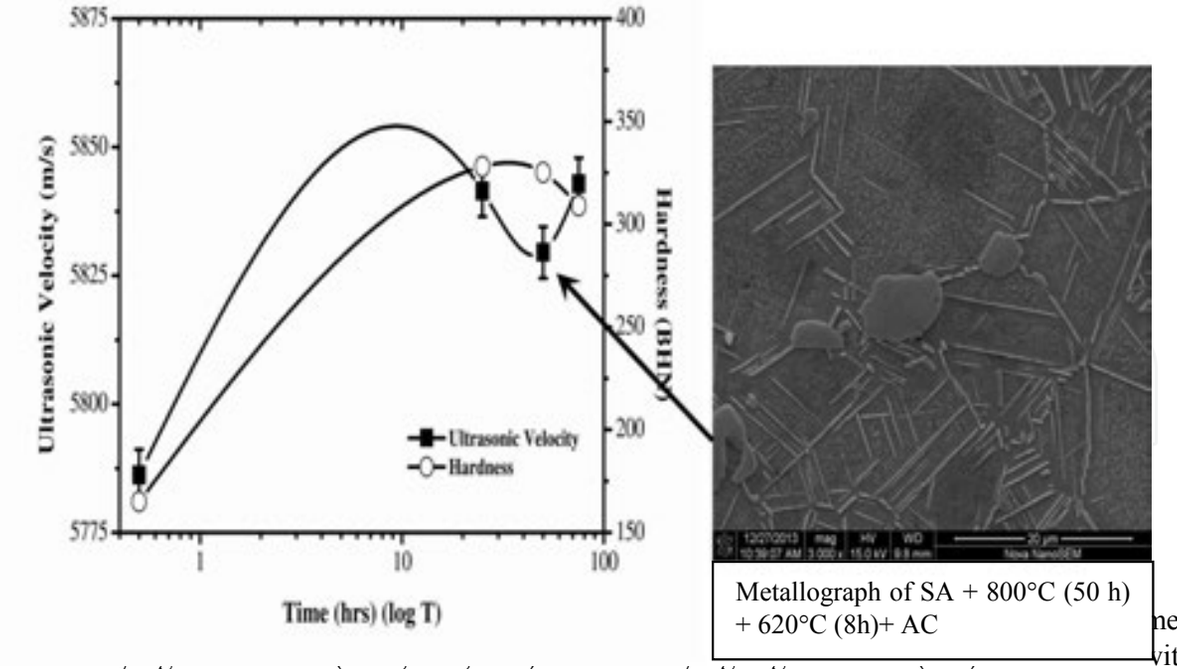


**Figure 15.** Ultrasonic Velocity and Hardness vs. Time for Solution Annealed (SA) specimen thermally aged at 800°C (25 h,50 h,75 h) followed by ageing at 620ºC (8 h) and studied with respect to the readings of SA specimen

Figure 15. Ultrasonic Velocity and Hardness vs. Time for Solution Annealed (SA) specimen thermally aged at 800°C (25 h,50 h,75 h) followed by ageing at 620ºC (8 h) and studied with respect to the readings of SA specimen

http://dx.doi.org/10.5772/61119

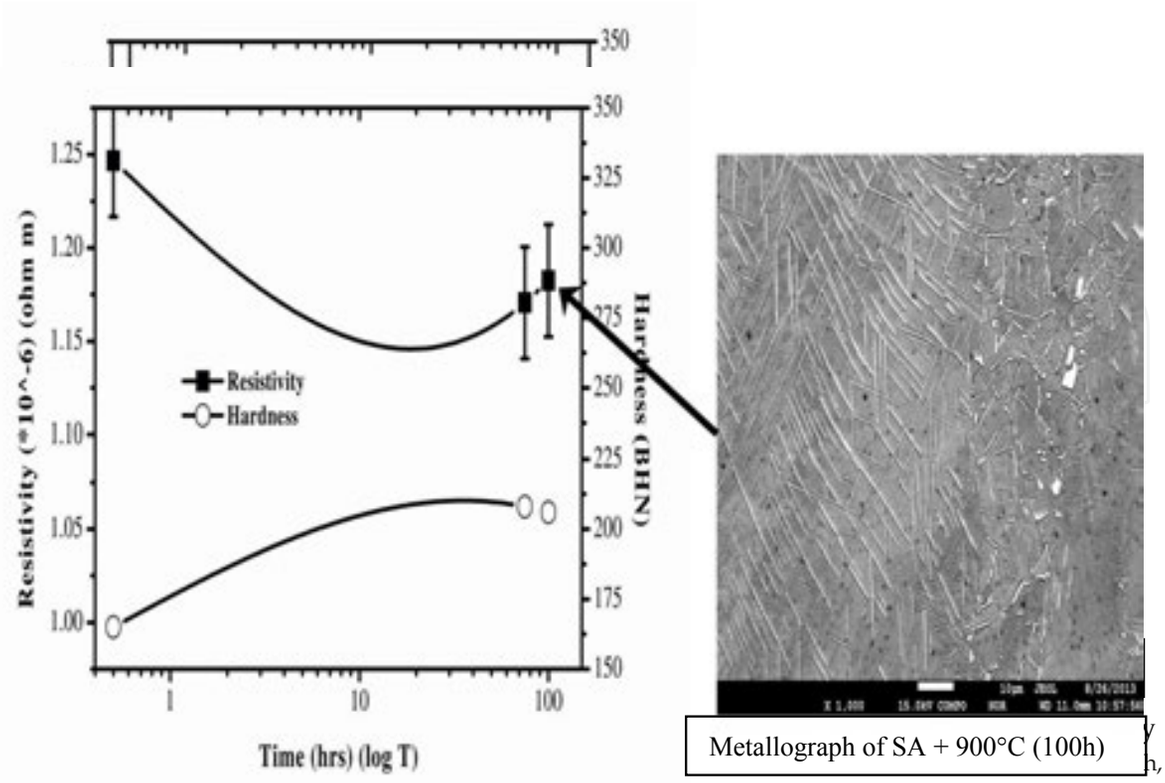


Fi h, 100 h) and studied with respect to the readings of SA specimen

**Figure 16.** Resistivity and Hardness vs. Time for Solution Annealed (SA) specimen thermally aged at 900°C (75 h, 100 h) and studied with respect to the readings of SA specimen

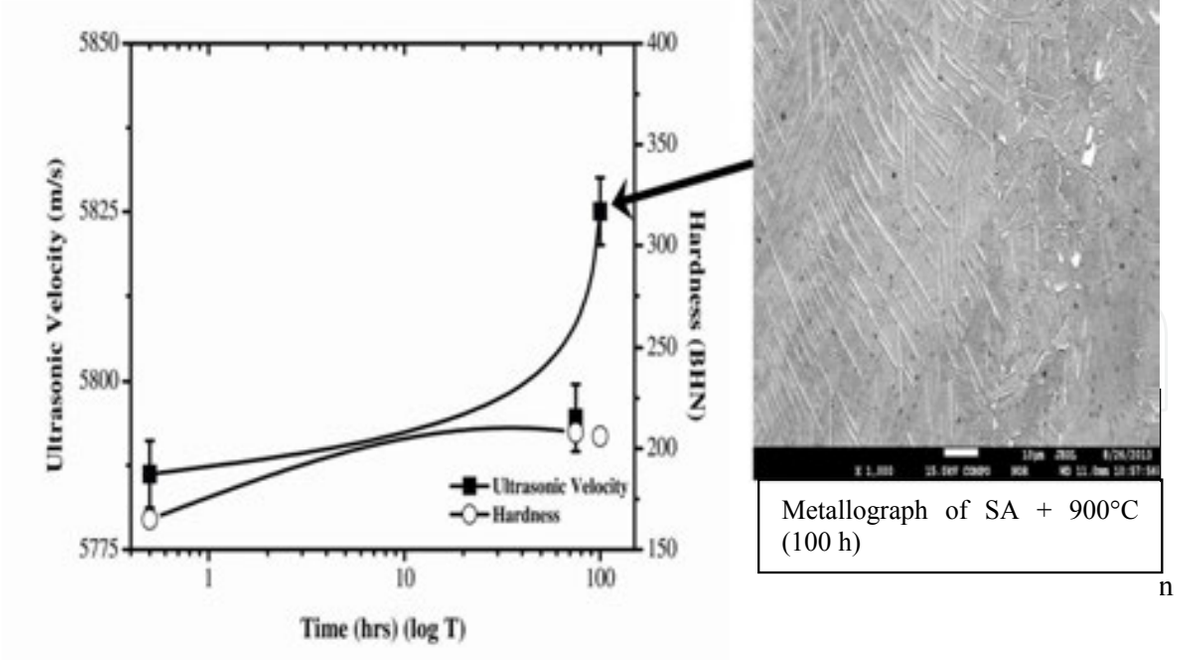


n

**Figure 17.** Ultrasonic Velocity and Hardness vs. Time for Solution Annealed (SA) specimen thermally aged at 900°C (75 h, 100 h) and studied with respect to the readings of SA specimen

Figure 17. Ultrasonic Velocity and Hardness vs. Time for Solution Annealed (SA) specimen thermally aged at 900°C (75 h, 100 h) and studied with respect to the readings of SA specimen

## 5. Conclusions

From the experimental study it is found that resistivity is sensitive to the structural variations that occur on ageing and ultrasonic velocity is more sensitive towards initial formation of fine precipitates and during their nucleation and growth, while hardness is only affected after the formation of the precipitates to a critical size which can hinder the dislocation movement. There will be considerable distortion of the matrix due to the presence of the coherent phase having lattice parameters different from those of the solvent and this distortion will extend over a distance more than the size of precipitate. It is this distortion that interferes with the movement of dislocations and accounts for the increase in hardness and strength during ageing. These observations are consistent with electron microscopy studies.

## Acknowledgements

This work was carried out at CSIR-National Metallurgical Laboratory (NML), Jamshedpur. The authors thank the Director, CSIR-National Metallurgical Laboratory (NML) for his kind permission to carry out and publish this work.

## Author details

V. Acharya, S. Ramesh and G.V.S. Murthy*

*Address all correspondence to: gvs@nmlindia.org

Materials Science and Technology Division, CSIR- National Metallurgical Laboratory, Jamshedpur, India

## References

[1] Roger C. Reed. *The Superalloys: Fundamentals and Applications*. Cambridge University press; 2006, pp. 1-101.

[2] Matthew J. Donachie and Stephen J. Donachie. *Superalloys: A Technical Guide*. 2nd edn., ASM International; 2002.

[3] Sims C.T. and Hagel W.C. *The Superalloys*. Wiley, New York; 1972.

[4] Sims C.T., Stoloff N.S. and Hagel W.C. *Superalloys II*. Wiley, New York; 1987.

[5] Åsa Martinsson. *Ageing Influence on Nickel-Based Superalloys at Intermediate Temperatures (400ºC-600ºC)*. Master Thesis. Luleå University of Technology; 2006.

[6] Collins H.E. and Quigg R.J. 'Carbide and Intermetallic Instability in Advanced Nickel-Base Superalloys', *ASM Trans. Quart*., March 1968, L6 1, pp. 139.

[7] Dieter G.E. *Mechanical Metallurgy*. McGraw-Hill Book Co., London; 1988.

[8] Martin J.W. *Precipitation Hardening*. Pergamon Press, New York; 1968.

[9] Sidney H. Avner. *Introduction to Physical Metallurgy*, 2nd edn., Tata McGraw-Hill Education; December 1997.

[10] Rajan T.V., Sharma C.P. and Ashok Sharma. *Heat Treatment: Principles and Techniques*. 2nd edn. PHI learning Pvt. Ltd.; 2011.

[11] Stanley R.K., Moore P.O. and McIntire P. (eds.). *Nondestructive Testing Handbook*, 2nd edn., vol. 9, Special Nondestructive Testing Methods, American Society for Nondestructive Testing, Columbus, OH,1995.

[12] Baldev Raj, Jayakumar T. and Thavasimuthu M., *Practical Non-Destructive testing*, 3rd edn., Narosa Publishing House Pvt. Ltd., 2011.

[13] Metals Handbook: *Mechanical Testing*, 9th edn., vol. 8.

[14] Metals Handbook: *Non-Destructive Evaluation and Quality Control*, 9th edn., vol. 17.

[15] Victor Giurgiutiu and Adrian Cuc, 'Embedded Non-destructive Evaluation for Structural Health Monitoring, Damage Detection, and Failure Prevention', Sage Publications, *The Shock and Vibration Digest*, March 2005, vol. 37, no. 2, pp. 83-105.

[16] Farrar C.R. and Worden K. 'An Introduction to Structural Health Monitoring', *Proc Trans Royal Soc A*, 2007, 365, pp. 303-315.

[17] Nanekar P.P. and. Shah B.K. 'Characterization of Material Properties by Ultrasonic", *BARC Newsletter*, Issue No. 249.

[18] Thompson R.B. 'Theory and Application of Ultrasonic Microstructural Characterization', *J Minerals Metals Mater Soc* (*TMS*) (*JOM*), October 1992.

[19] Eds. Buck O. and Wolf. S.M., *Nondestructive Evaluation: Application & Materials Processing*, Materials Park, OH: ASM, 1984.

[20] Wadley H.N.G. (ed.). *NDE of Microstructure for Process Control*, Materials Park, OH: ASM, 1985.

[21] Bobo S.P. *Review of Progress in Quantitative Nondestructive Evaluation*, vol. 9B, Thompson D.O. and Chimenti D.E. (eds.), New York: Plenum Press, 1990, pp. 2097-2169.

[22] Eds. Thompson D.O. and Chimenti. D.E. *Review of Progress in Quantitative Nondestructive Evaluation*, vol. 1-11, New York: Plenum Press, pp. 1982-1992.

[23] Ruud C.O. and Green R.E. Jr. (eds.). *Nondestructive Methods for Materials Property Determination*, New York: Plenum Press, 1984.

[24] Bussiere J.F. (ed.). *Nondestructive Characterization of Materials II*, New York: Plenum Press, 1987.

[25] Holler P. (eds.). *Nondestructive Characterization of Materials*, Berlin: Springer-Verlag, 1989.

[26] Buck O. and Wolf S.M. (eds.). *Nondestructive Evaluation: Microstructural Characterization and Reliability Strategies*, Warrendale, PA: TMS, 1981.

[27] Liaw P.K., Buck O. and Wolf S.M. (eds.). *Nondestructive Evaluation and Material Properties of Advanced Materials*, Warrendale, PA: TMS, 1991.

[28] Baikand J.M. and Thompson R.B. *J Nondestruct Eval*, 4, 1984, pp. I77-196.

[29] Margetan F.J., Thompson R.B. and Gray T.A. *J Nondestruct Eval*, 7, 1988, pp. 131-152.

[30] Nagy P.B. and Adler L. *Review of Progress in Quantitative Nondestructive Evaluation*, Thompson D.O. and Chimenti D.E. (eds.), New York: Plenum Press, 1991, vol. 10A, pp. 177-184.

[31] Yalda-Mooshabad I., et al. *J Nondestruct Eval*.

[32] Giurgiutiu V. and Cuc A., 'Embedded Non-destructive Evaluation for Structural Health Monitoring, Damage Detection, and Failure Prevention', Sage Publications, *The Shock and Vibration Digest*, March 2005, vol. 37, no. 2, pp. 83-105.

[33] *Analytical Ultrasonic in Material Research and Testing*, NASA CP 2383, 1984.

[34] Banerjee S. and Shah B.K. 'Characterization of Industrial Materials', In G. Sridhar, S. Ghosh Chowdhary and N.G. Goswami (eds.), *Material Characterization Techniques – Principles and Applications*, 1999, pp. 1-15.

[35] Dobmann G., et al. 'Non-Destructive Characterization of Materials: A Growing Demand for Describing Damage and Service Life Relevant Ageing Process in Plant Components', *Nucl Engin Design*, 1997, vol. 171, pp. 95-112.

[36] Thomson R.B. 'Laboratory Non-Destructive Evaluation Technology Material Characterization', *J Non-Destruct Eval*, 1996, vol. 15, no. 3 & 4.

[37] Raj B., et.al. 'NDE Methodologies for Characterization of Defects, Stresses and Microstructure in Pressure Vessels and Pipes', *Int J Pressure Vessel Piping*, September 1997, vol. 73, issue 2, pp. 133-146.

[38] Shah D.N. 'Testing and Characterization of Materials', Workshop, IIM, Mumbai Chapter, 1990.

[39] Shah B.K. 'Advances in NDT Techniques for Flaw and Materials Characterization', Seminar, IIM, Mumbai Chapter, 1992.

[40] Mitra A. (ed.) 'Recent Trends in Nondestructive Evaluation of Materials', Workshop, 1997.

[41] Bhattacharya D.K. 'Characterization of Microstructure in Steels by Magnetic Techniques an Overview', *ISNT J Non-Destructive Eval*, 1997, vol. 17, no. 1.

[42] Dobmann G. et.al. 'Ageing Material Evaluation and Studies by Non-Destructive Techniques (AMES-NDT), A European Network Project', *J Nucl Engin Design*, 2001, vol. 206, pp. 363-374.

[43] Theiner W.A., et.al. 'Non-Destructive Analysis of the Structure of Pressure Vessel Steels by Micro-magnetic Testing Techniques', *J Nucl Engin Design*, December 1983, vol. 76, issue 3, pp 251-260.

[44] Willems H. and Gobbeles K. 'Characterization of Microstructure by Backscatter Ultrasonic Waves', *Mat Sci*, November- December 1981, vol. 15, pp. 549-553.

[45] Mak D.K. 'Determination of Grain Size, Hysteresis Constant and Scattering Factor of Polycrystalline Material Using Ultrasonic Attenuation', *Canadian Metall Quart*, vol. 25, no.3, pp 253-255.

[46] Diamand R.D. 'Development of Instrument for On-Line Measurement of Grain Size in Copper Alloys and Stainless Steels', 21st Annual British Conference on Non-Destructive Testing NDT 0 86, pp. 225-242.

[47] Badidi Bouda A., et.al. 'Grain Size Influence on Ultrasonic Velocities and Attenuation', *Proc of NDT & E International*, January 2003, vol. 36, 1, pp. 1-5.

[48] Generazio E.R. 'Ultrasonic Attenuation Measurements to Determine Onset, Degree and Completion of Recrystallization', *Mater Eval*, August 1998, vol. 46, pp. 1198-1203.

[49] Murthy G.V.S., Sridhara G., Anish Kumar and Jayakumar T. 'Characterization of Intermetallic Precipitates in a Nimonic Alloy by Ultrasonic Velocity Measurements', *Mater Character*, March 2003, vol. 60, no. 3, pp 234-239.

[50] Nanekar P.P., et.al. 'Non-Destructive Characterization of Ceramics and Concrete Structure', Testing and Quality Control, conducted by ASM India Section, May 2001, Mumbai.

[51] Smith R.L., et.al. "Ultrasonic Attenuation, Microstructure and Ductile to Brittle Transition Temperature in Fe-C Alloys", *Mater Eval*, February 1983, vol. 41, pp. 219-222.

[52] Vary A. 'Concepts for Interrelating Ultrasonic Attenuation, Microstructure and Fracture Toughness in Polycrystalline Solids', *Mater Eval*, April 1988, vol. 46, pp. 642-649.

[53] Jean F. Bussiere, et.al. 'Analysis of the Effect of Graphite Morphology on the Elastic Properties of Cast Iron', Proc. of 3rd Symposium on Non-Destructive Characterization of Materials, October 1988, Saarbrucken, FRG, pp. 353-660.

[54] Shah B.K., et.al. 'Qualification of Beta Heat Treatment of Uranium Fuel Rods by Ultrasonic', *Insight, J British Instit Non-destruct Testing*, November 1999, vol. 41, no. 11, pp. 707-709.

[55] Nanekar P.P., et al. 'Ultrasonic Characterization of Precipitation Hardenable 17-4 PH Stainless Steel', Proc. of 47th Annual technical meeting of Indian Institute of Metals, Hyderabad, November 1993.

[56] Weston-Bartholomew W. 'Use of Ultrasonic Goniometer to Measure Depth of Case Hardening', *Int Adv Nondestruct Testing* 1979, vol. 6, pp. 111-123.

[57] Y. Lu, Parthasarathi S. and Wadley H.N.G. 'Advanced Sensing, Modeling And Control Of Materials Processing', In Matthys E.F. and Kushner B. (eds.), Warrendale, PA: TMS, 1992, pp. 204-221.

[58] Margetan F.J. and Thompson R.B. *Review of Progress in Quantitative Nondestructive Evaluation 1992*, D.O. Thompson and D.E. Chimenti (eds.), vol. 11B, New York: Plenum Press, pp. 1717-1724.

[59] Thompson R.B. et al. *Review of Progress in Quantitative Nondestructive Evaluation 1992*, D.O. Thompson and D.E. Chimenti (eds.), vol. 11B, New York: Plenum Press, pp. 1685-1691.

[60] 'On-Line Monitoring of Sheet Metal Texture', *J of Nondestruct Eval*.

[61] Green R.E., et.al. 'Ultrasonic and Acoustic Emission Detection of Fatigue Damage', *Int Adv Nondestruct Testing*, 1979, vol. 6, pp. 125-177.

[62] Joshi N.R. and Green R.E. 'Ultrasonic Detection of Fatigue Damage', *Fract Mech* 4, 1972, pp. 577-583.

[63] Gerd Dobmann, et.al. 'Nondestructive Characterization of Materials (Ultrasonic And Magnetic Techniques) For Strength And Toughness Prediction And The Detection Of Early Creep Damage', *Nucl Engin Design*, 1992, 157, pp. 137-158.

[64] Birring A.S., et al. 'Ultrasonic Detection of Hydrogen Attack in Steels', *Corrosion*, vol. 45, no. 3, pp. 259-263.

[65] Kruger S.E., et al. 'Hydrogen Damage Detection by Ultrasonic Spectral Analysis', Proc. of NDT & E International, 1999, vol. 32, pp. 275-281.

[66] Shah B.K. 'Monitoring of Intergranular Corrosion in Austenitic Stainless Steels AISI 304 by Non-Destructive Testing Methods', M.Tech Thesis, IIT Bombay, 1984.

[67] Ikuta E., et al. 'Ultrasonic Evaluation of Thermal Embrittlement', Proc. of the 13th International Conference in the Nuclear and Pressure Vessel Industries, Kyoto, Japan, 1985, pp. 285-289.

[68] Shah B.K, et.al. 'Ultrasonic Characterization of Ageing Degradation During Long Term High Temperature Exposure in Nickel Base Alloy 625', Proc. of 14th World Conference on NDT, New Delhi, December 1996, pp. 2235-2238.

[69] Bowler N. 'Theory of Four-Point Direct Current Potential Drop Measurements on a Metal Plate', *Proc Trans. Royal Soc A*, 2007, 463, pp. 817-836.

[70] Panseri C. and Federighi T. *J Instit Metals*, 1966, vol. 94, pp. 99-107.

[71] Kasap S. O. *Principles of Electronic Materials and Devices*, 2nd edn., Tata McGraw-Hill, Boston 2002.

[72] Dubost B., Bouvaist J. and Reboul M. 'Aluminum Alloys: Their Physical and Mechanical properties', *Engin Mater Advis Serv Ltd*., Chalottesville, 1986, vol. 2, pp. 1109-1123.

[73] Blitz. J. 'Electrical and Magnetic Methods of Non-Destructive Testing', Springer, 1997, vol. 3.

[74] Papadakis E.P. 'Ultrasonic Velocity and Attenuation Measurement Methods with Scientific and Industrial Applications', *Physic Acoust*, 1976, vol. 12, pp. 277-374.

[75] Holbrook J. and Bussiere J.F (eds.). *Nondestructive Monitoring of Materials Properties*, Pittsburgh, PA: MRS, 1989.

[76] Wadley H.N.G., et al. (eds.). *Intelligent Processing of Materials and Advanced Sensors*, Warrendale, PA: TMS, 1987.

[77] Wadley H.N.G. and Eckhart W.E., Jr. (eds.). *Intelligent Processing of Materials*, Warrendale, PA: TMS, 1990.

[78] Matthys E.F. and Kushner B. (eds.). *Advanced Sensing, Modeling and Control of Materials Processing*, Warrendale, PA: TMS, 1992.

[79] Zhao J.C. and Henry Michael F. 'The Thermodynamic Prediction of Phase Stability in Multi Component Superalloys. *JOM*, 2002; pp. 37-40.

[80] Chandrasekar R., Chester C.H. Lo, Frishman A.M., Larson B.F. and Nakagawa N. 'Quantification of Precipitates and Their Effects on the Response of Nickel-base Superalloy to Shot Peening', AIP Conf. Proc. 1430, 2012, pp. 1437-1444.

IntechOpen